Available online at www.sciencedirect.com

ScienceDirect

IFAC PapersOnLine 55-14 (2022) 40–45

Centralized Multi-Sensor Poisson Multi-Bernoulli Mixture Tracker for Autonomous Driving

Hyerim Lee * **Jaeho Choi** ** **Sejong Heo** *** **Kunsoo Huh** **

* *Department of Automotive Engineering (Automotive-Computer Convergence), Hanyang University, Seoul, Korea, (e-mail: rim7951@hanyang.ac.kr).*
** *Department of Automotive Engineering, Hanyang University, Seoul, Korea, (e-mail: jaeho0608, khuh2@hanyang.ac.kr).*
*** *Hyundai Motor Company, Seoul, Korea, (e-mail: sejong.heo@hyundai.com).*

Abstract: With recent advances in Advanced Driver Assistance Systems (ADAS), autonomous driving has increased the need for reliable perception techniques. To achieve reliability, automotive sensors are being applied to autonomous driving vehicles, such as cameras, LiDAR, and radars. Various methods for fusing sensors have been studied to increase performance. In this study, we propose a centralized multi-sensor tracker, which is a first attempt to take advantage of fusing heterogeneous onboard sensors while accounting for data uncertainties. The proposed approach uses a Random Finite Set based Poisson Multi-Bernoulli Mixture filter. Experimental results from an actual vehicle dataset show that the proposed method tracks accurately even when objects are occluded or overlapped. It demonstrates the capability of tracking objects for autonomous driving in an urban environment.

Keywords: Advanced Driver Assistance Systems, Multi-Sensor Fusion, Multi-Object Tracking, Poisson Multi-Bernoulli Mixture Filter, Random Finite Set.

1. INTRODUCTION

In autonomous driving, it is necessary to adequately perceive the complex surrounding environment. Multi-object tracking is a particularly crucial part. If tracking results are poor, it may have an impact on subsequent path prediction and vehicle control parts. The purpose of multi-object tracking is to jointly predict the state and the number of objects. However, performing multi-object tracking well is quite tough due to the following difficulties: random ordering and cardinality of objects and observations; detection uncertainty; and data associations.

There are three common filter-based approaches to dealing with the problem of multi-object tracking that have the greatest impact on performance. The Joint Probabilistic Data Association (JPDA), introduced in Bar-Shalom et al. (2009), is a method of creating every possible association matrix between observations and previously detected objects. The observation is associated with a high probability when the position of the observation is close to the track. As a result, the association with the highest probability is chosen as an estimation. Multiple Hypothesis Tracking (MHT) in Reid (1979) holds multiple data association hypotheses, unlike the JPDA, which returns the one with the highest probability as the estimation result. Because all possible tracks are preserved and updated, it's especially useful when the motion model uncertainty exists. The MHT is used in many applications along with hypothesis reduction as it may have exponential growth in the number of hypotheses. Due to practical and fundamental necessity, Mahler (2007) introduces the Random Finite Set (RFS). It allows for a Bayesian approach to multi-object tracking as the RFS can naturally model uncertainties accurately.

Among the RFS-based algorithms, the Poisson Multi-Bernoulli Mixture (PMBM) filter of García-Fernández et al. (2018) has demonstrated superior performance with a low computational cost. The PMBM filter has three distinguishing features. The PMBM density has a conjugacy property, which means that both the posterior and prior distributions have the same functional form. It is clearly explained in García-Fernández et al. (2018). Another is that it divides tracking objects into undetected and detected objects when estimating them. Because the PMBM is under a detection-based tracking framework, it cannot explicitly track undetected objects, but it does represent their possibility. The other is that it can estimate the state of objects elegantly even when objects are occluded by keeping track of all feasible data association hypotheses throughout time. However, because this is computationally intensive, the PMBM filter is accompanied by several reduction strategies.

Aside from the approaches explained above, as interest in deep learning has increased recently, deep-learning based tracking method research has grown. Deep Learning is being used to extract features from raw sensor data using a complicated network rather than directly using object-level sensor data as Scheidegger et al. (2018) or to track in

Peer review under responsibility of International Federation of Automatic Control.
10.1016/j.ifacol.2022.07.580

an end-to-end way as Frossard and Urtasun (2018). It has good potential, but its tracking performance is comparable to or slightly inferior to filter-based tracking methods, and it necessitates training. Therefore, computational cost must be a burden for autonomous vehicle applications. Furthermore, it lacks flexibility in parameter tuning, and thus it is not robust to changes in the environment and sensor setup.

In autonomous vehicle applications, various types of onboard automobile sensors, such as cameras, LiDAR, and radar sensors, are used to observe surrounding environments. As each sensor has its own set of benefits and drawbacks, we need to fuse them to increase the accuracy of the object state estimations. This paper chooses a centralized sensor fusion architecture introduced in Hall and Llinas (1997) that fuses measurements from each sensor and uses a single state estimator. It allows a central filter to take entire responsibility for fusing the data.

Several previous multi-object tracking approaches based on the PMBM filter have been proposed. Pang et al. (2021) and Pang and Radha (2021) propose single-sensor PMBM trackers that use neural networks to make LiDAR raw data into 3D detection measurements. Fröhle et al. (2018) employs heterogeneous multi-sensors, but they use GNSS and V2F, not the sensors mainly used in general autonomous driving. Thanh et al. (2021) uses multiple automotive sensors in a decentralized PMBM tracker, which updates as each sensor data arrives. It conducts an evaluation using an automated driving simulation toolbox.

This paper develops a centralized filter-based multi-sensor tracking algorithm for the autonomous vehicle. To the best of our knowledge, this is the first attempt at fusing multiple heterogeneous onboard sensors for multi-object tracking. The contributions of the paper can be summarized as follows: (1) propose a tracking algorithm using a Poisson Multi-Bernoulli Mixture (PMBM) filter with multi-sensor fusion concerning data uncertainties. (2) implement using linear and gaussian models. (3) assess performance using actual vehicle driving data.

The remainder of the paper is organized as follows. In Chapter 2, we introduce the background information for this paper and we propose a centralized tracking algorithm in Chapter 3. We suggest how multiple sensors' data are fused in detail. In Chapter 4, we evaluate the proposed algorithm based on an actual vehicle dataset and discuss experimental results.

2. BACKGROUND

In this section, background information for the paper is given. Mathematical symbols can be found in Table 1. Other symbols that aren't in the table are additionally explained.

2.1 Random Finite Set

A Random Finite Set (RFS), also known as a Point Process, is a set with random cardinality and ordering states. RFS can model states and observation uncertainty naturally by treating them as random variables.

Table 1. Nomenclature

Mathematical Symbols	Meaning
x	Object state
$\mathbf{x}$	Object RFS
$\mathbf{x}^u$	Undetected object RFS
$\mathbf{x}^d$	Detected object RFS
$\biguplus$	Disjoint Union
z	Measurement state
$\mathbf{z}$	Measurements RFS
p_s	Survival probability
p_d	Detection probability
r	Existence probability
λ_p	Poisson rate
λ_c	Clutter rate
$\mathcal{N}(\cdot)$	Gaussian function
w	Hypothesis weight
$p(\cdot)$	Probability density function
$f^{\mathcal{P}}(\cdot)$	Poisson RFS density
$f^{\mathcal{MBM}}(\cdot)$	MBM RFS density

Poisson RFS intensity is defined as $\mu(x) = \lambda_p p(x)$ where Poisson distributed with rate λ_p and independent and identically distributed (i.i.d.) $p(x)$. Poisson RFS density $f^{\mathcal{P}}(\mathbf{x})$ is

$$f^{\mathcal{P}}(\mathbf{x}) = e^{-\mu(x)} \prod_{x\in\mathbf{x}} \lambda_p p(x). \tag{1}$$

A Bernoulli RFS density is expressed as

$$f^{\mathcal{B}}(\mathbf{x}) = \begin{cases} 1-r, & \mathbf{x} = \emptyset \\ rp(x), & \mathbf{x} = \{x\} \\ 0, & |\mathbf{x}| \geq 2. \end{cases} \tag{2}$$

where r denotes an existence probability and $p(x)$ is a probability density function if an object exists.

A Multi-Bernoulli (MB) RFS density is the disjoint union of the independent Bernoulli RFSs.

$$f^{\mathcal{MB}}(\mathbf{x}) = \sum_{\biguplus_{i\in\mathcal{I}} \mathbf{x}_i = \mathbf{x}} \prod_{i\in\mathcal{I}} p_i(\mathbf{x}_i) \tag{3}$$

where $\mathcal{I}$ denotes a set of objects. It is used as the set of potential objects $\{(r_i, p_i(x))\}_{i\in\mathcal{I}}$ that include the existence probabilities of an object r_i and the distribution of its states $p_i(x)$.

A Multi-Bernoulli Mixture (MBM) RFS density is the weighted sum of MB RFS densities. MBM RFS density is used in handling a situation where we have multiple data association hypotheses.

$$f^{\mathcal{MBM}}(\mathbf{x}) = \sum_{j\in\mathcal{J}} w_j \sum_{\biguplus_{i\in\mathcal{I}^j} \mathbf{x}_i = \mathbf{x}} \prod_{i\in\mathcal{I}^j} p_{j,i}(\mathbf{x}_i). \tag{4}$$

where $\mathcal{J}$ stands for hypotheses sets. MBM RFS parameters are $\{w^d_{j,i}, \{r^d_{j,i}, p^d_{j,i}(x)\}_{i\in\mathcal{I}}\}_{j\in\mathcal{J}}$, where $w^d_{j,i}$ denotes the weight of the i th detected object of the j th hypotheis, existence probability $r^d_{j,i}$, and state distribution $p^d_{j,i}(x)$. Each weight determines the likelihood that the hypothesis will occur.

2.2 Poisson Multi-Bernoulli Mixture filter

Poisson Multi-Bernoulli Mixture (PMBM) RFS density is represented by a convolution of Poisson RFS density and Multi-Bernoulli Mixture RFS density given by

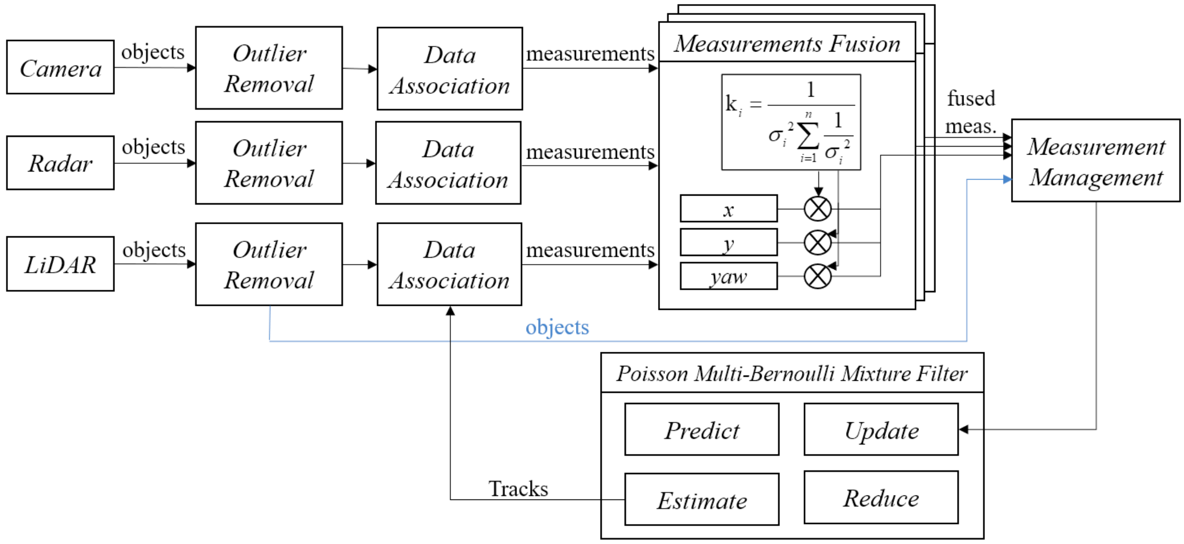

Fig. 1. The architecture of the proposed method. The tracker consists of four components: Data Association (DA), Measurement Fusion (MF), Measurement Management (MM), and Filtering with the PMBM filter.

$$f^{\mathcal{PMBM}}(\mathbf{x}) = \sum_{\mathbf{x}^u \uplus \mathbf{x}^d = \mathbf{x}} f^{\mathcal{P}}(\mathbf{x}^u) f^{\mathcal{MBM}}(\mathbf{x}^d). \tag{5}$$

The object set $\mathbf{x}_t$ at time t is the union of two disjoint sets, the undetected and detected object sets.

$$\mathbf{x}_t = \mathbf{x}_t^u + \mathbf{x}_t^d \tag{6}$$

$\mathbf{x}_t^u$ and $\mathbf{x}_t^d$ denotes the set of undetected objects at time t modeled by the Poisson RFS and the set of detected objects modeled by the MBM RFS, respectively. Poisson RFS density and MBM RFS density are independently predicted and updated during the PMBM recursion.

To cope with data association, the PMBM uses local hypotheses and global hypotheses. Local hypotheses are a set of data associations for a particular object from the beginning of tracks to the present. A possible combination of local hypotheses is referred to as global hypotheses. Global hypotheses contain the data associations of all objects. As a result, keeping a reasonable number of hypotheses is crucial to obtaining a favorable computational cost.

3. PROPOSED METHOD

3.1 Architecture

The architecture of the proposed method is shown in Fig. 1. After outliers of each sensor are removed, data associations for each sensor with regard to tracks are implemented. There will be no more than one measurement for an object per sensor. Following that, the associated measurements are fused at the MF step. By taking into account the data uncertainty, the proposed method combines several sensors with appropriate weights. It allows the tracker to complement the limits of each sensor, resulting in more accurate tracking results in dynamic conditions. We will go through weight calculations in detail in the next section. To compensate for measurement loss due to the data association with previously detected tracks, LiDAR data is included in the measurements set to initiate the newborn track at MM. Finally, these measurement sets are utilized at the update step of the PMBM filter. Filtering output is used at track-to-sensor data association as tracks and this process is done recursively.

3.2 Uncertainty-aware Measurement Fusion

To get appropriate weight to fuse, we adopt the weight calculations of Liu et al. (2020) and modify them to be used for multi-sensor multiple data fusion. Weights α concerning the uncertainty of sensor data are derived as follows:

An objective function is defined as

$$\begin{aligned} f(\alpha) &= \sum_{i=1}^{n} \alpha_i^2 \sigma_i^2 \\ \textit{subject to} & \sum_{i=1}^{n} \alpha_i = 1 \end{aligned} \tag{7}$$

where n denotes the number of sensors or data types. Using the Lagrangian multiplier method, the Lagrangian function is expressed as

$$L(\alpha) = f(\alpha) + v\left(\sum_{i=1}^{n} \alpha_i - 1\right) \tag{8}$$

where v denotes the Lagrange multiplier. The partial derivative α_i of the Lagrangian function (8) is as follows:

$$\begin{aligned} \frac{\partial L}{\partial \alpha_i} &= \frac{df}{d\alpha_i} + v \\ &= 2\alpha_i \sigma_i^2 + v. \end{aligned} \tag{9}$$

Setting $\frac{\partial L}{\partial \alpha_i} = 0$ to obtain the minimum value, α_i and v are

$$\alpha_i = \frac{v}{2\sigma_i^2}, \quad v = \frac{2}{\sum_{i=1}^{n} \frac{1}{\sigma_i^2}} \tag{10}$$

The fusion weight of each sensor data i is α_i as

$$\alpha_i = \frac{1}{\sigma_i^2 \sum_{i=1}^{n} \frac{1}{\sigma_i^2}}. \tag{11}$$

This weight calculation is used not only for each sensor but also for each sensor data type. Under the same given observations, equally-weighted measurement fusion cannot predict a track center. However, if the uncertainty of each sensor is taken into account while fusing them using weights computed by (7)-(11), more accurate fused outputs are obtained and the tracker can achieve better performance than the equally-weighted output.

3.3 Filtering with PMBM filter

The prediction, update, estimation, and reduction parts of the PMBM filter are all discussed in depth. We note that all the explanations below and the implementation of the proposed method use linear and Gaussian models. The PMBM predicts and updates Poisson RFS and MBM RFS independently.

Prediction A target has a p_s chance of surviving and moving with a transition density $g(\cdot)$, or $1-p_s$ chance of dying. Various motion models can be used to represent the transition density as $g(\mathbf{x}|\mathbf{y}) = \mathcal{N}(\mathbf{x}; \mathbf{F}\mathbf{y}, \mathbf{Q})$. Target birth is modelled by Poisson RFS with intensity $\lambda^b(\cdot)$

$$\lambda^b(\mathbf{x}) = \sum_{i=1}^{N_b} w_{b,i}^u \mathcal{N}(\mathbf{x}; \bar{\mathbf{x}}_{b,i}^u, \mathbf{\Sigma}_{b,i}^u) \tag{12}$$

where N_b denotes the number of births. Poisson RFS intensity is predicted as

$$\mu_{t|t-1}(\mathbf{x}) = \lambda_t^b(\mathbf{x}) + p_s \sum_{i=1}^{N_u} w_{u,i} \mathcal{N}(\mathbf{x}; \mathbf{F}\bar{\mathbf{x}}_{u,i}^u, \mathbf{F}\mathbf{\Sigma}_{u,i}^u \mathbf{F}^T + \mathbf{Q}). \tag{13}$$

The components of the MBM RFS are hypothesis weight, probability of existence, and probability density function. The hypothesis weight $w_{t|t-1}^{j,i}$ does not change since no measurement is taken at this point. The probability of existence $r_{t|t-1}^{j,i}$ is predicted to be $r_{t-1|t-1}^{j,i} p_s$. Prediction of the probability density function $p_{t|t-1}^{j,i}(\mathbf{x})$ is

$$p_{t|t-1}^{j,i}(\mathbf{x}) = \mathcal{N}(\mathbf{x}; \mathbf{F}\bar{\mathbf{x}}_{j,i}^d, \mathbf{F}\mathbf{\Sigma}_{j,i}^d \mathbf{F}^T + \mathbf{Q}) \tag{14}$$

where i denotes the Bernoulli component and j a global hypothesis index.

Update Each measurement at time t might be a first detection, a detection of a previously detected target, or clutter. Targets are detected with probability p_d and created with density $l(\cdot|\mathbf{x})$, or they are missed with probability $1-p_d$. Measurement likelihoods are $f(\mathbf{z}|\mathbf{x}) = \mathcal{N}(\mathbf{z}; \mathbf{H}\mathbf{x}, \mathbf{R})$. The PMBM update has three step: the Poisson RFS update, MBM RFS update, and global hypotheses update.

In the Poisson RFS update, the states and variances of Poisson distribution will not change and intensity will be reduced as

$$\mu_{t|t}(\mathbf{x}) = (1-p_d)\mu_{t|t-1}(\mathbf{x}). \tag{15}$$

In the case of the MBM RFS update, new potential tracks that are detected for the first time are made from survived components after gating Poisson components on measurements

$$r_{t|t}^u(\mathbf{z}) = \frac{e(\mathbf{z})}{\rho^u(\mathbf{z})} \tag{16}$$

$$w_{t|t}^u(\mathbf{z}) \propto w_{t|t-1}^u \mathcal{N}(\mathbf{z}; \mathbf{H}\bar{\mathbf{x}}_{u,i}^u, S_{u,i}) \tag{17}$$

$$p_{t|t}^u(\mathbf{x}|\mathbf{z}) = \frac{p_d f(\mathbf{z}|\mathbf{x}) \mu_{t|t-1}(\mathbf{x})}{e(\mathbf{z})} \tag{18}$$

$$= \sum_{i=1}^{N_u} w_i(\mathbf{z}) \mathcal{N}(\mathbf{x}; \hat{\mathbf{x}}_{u,i}(\mathbf{z}), \hat{\mathbf{\Sigma}}_{u,i}) \tag{19}$$

where $c(\mathbf{z})$ denotes the clutter intensity and

$$\begin{aligned}
\rho^u(\mathbf{z}) &= e(\mathbf{z}) + c(\mathbf{z}) \\
e(\mathbf{z}) &= p_d \int f(\mathbf{z}|\mathbf{x}) \mu(\mathbf{x}) d\mathbf{x} \\
&= p_d \sum_{i=1}^{N_u} w_{u,i} \mathcal{N}(\mathbf{z}; \mathbf{H}\bar{\mathbf{x}}_{u,i}, S_{u,i}) \\
\hat{\mathbf{x}}_{u,i}(\mathbf{z}) &= \bar{\mathbf{x}}_{u,i}^u + \mathbf{\Sigma}_{u,i}^u \mathbf{H}^T S_{u,i}^{-1} (\mathbf{z} - \mathbf{H}\bar{\mathbf{x}}_{u,i}^u) \\
\hat{\mathbf{\Sigma}}_{u,i} &= (\mathbf{I} - \mathbf{\Sigma}_{u,i}^u \mathbf{H}^T S_{u,i}^{-1} \mathbf{H}) \mathbf{\Sigma}_{u,i}^u \\
S_{u,i} &= \mathbf{H} \mathbf{\Sigma}_{u,i}^u \mathbf{H}^T + \mathbf{R}.
\end{aligned} \tag{20}$$

Detected tracks without associated measurements are updated as

$$w_{t|t}^{j,i}(0) = w_{t|t-1}^{j,i}(1 - r_{t|t-1}^{j,i} + r_{t|t-1}^{j,i}(1-p_d)) \tag{21}$$

$$r_{t|t}^{j,i}(0) = \frac{r_{t|t-1}^{j,i}(1-p_d)}{1 - r_{t|t-1}^{j,i} + r_{t|t-1}^{j,i}(1-p_d)} \tag{22}$$

$$p_{t|t}^{j,i}(0) = p_{t|t-1}^{j,i}(\mathbf{x}). \tag{23}$$

When the track has associated measurements, the existence probability is set to 1, as it is considered to exist. The states and variances are updated by Bayesian update using associated measurements.

$$r_{t|t}^{j,i}(\mathbf{z}) = 1 \tag{24}$$

$$w_{t|t}^{j,i}(\mathbf{z}) = w_{t|t-1}^{j,i} r_{t|t-1}^{j,i} p_d \mathcal{N}(\mathbf{z}; \mathbf{H}\bar{\mathbf{x}}_{j,i}^d, S_{j,i}) \tag{25}$$

$$p_{t|t}^{j,i}(\mathbf{x}, \mathbf{z}) = \mathcal{N}(\mathbf{x}; \hat{\mathbf{x}}_{j,i}(\mathbf{z}), \hat{\mathbf{\Sigma}}_{j,i}) \tag{26}$$

where

$$\begin{aligned}
\hat{\mathbf{x}}_{j,i}(z) &= \bar{\mathbf{x}}_{j,i}^d + K_{j,i} S_{j,i}^{-1} (\mathbf{z} - \mathbf{H}\bar{\mathbf{x}}_{j,i}^d) \\
K_{j,i} &= \mathbf{\Sigma}_{j,i}^d \mathbf{H}^T \\
\hat{\mathbf{\Sigma}}_{j,i} &= \mathbf{\Sigma}_{j,i}^d - K_{j,i} S_{j,i}^{-1} K_{j,i}^T \\
S_{j,i} &= \mathbf{H} \mathbf{\Sigma}_{j,i}^d \mathbf{H}^T + \mathbf{R}.
\end{aligned} \tag{27}$$

After updating Poisson and MBM components, global hypotheses are updated by creating a cost matrix.

$$\begin{aligned}
C &= -ln \left[C_{old} \quad C_{new} \right]_{m \times (j+m)} \\
&= -ln \begin{bmatrix} \underbrace{\begin{matrix} c_o^{1,1} & \cdots & c_o^{1,j} \\ \vdots & \ddots & \vdots \\ c_o^{m,1} & \cdots & c_o^{m,j} \end{matrix}}_{j} & \underbrace{\begin{matrix} c_n^{1,1} & \cdots & 0 \\ \vdots & \ddots & \vdots \\ 0 & \cdots & c_n^{m,m} \end{matrix}}_{m} \end{bmatrix}_{m \times (j+m)} .
\end{aligned} \tag{28}$$

where c_o and c_n are the cost of old and newly detected targets. j and m denote the number of detected targets at the previous timestep and the number of measurements. The cost of the previously detected targets c_o is

$$c_o^{j,i} = \frac{w^{j,i} \rho^{j,i}(\mathbf{z})}{\rho^{j,i}(0)} = \frac{w^{j,i} r^{j,i} p_d \mathcal{N}(\mathbf{z}; \mathbf{H}\bar{\mathbf{x}}_{j,i}^d, S_{j,i})}{w^{j,i}(1 - r^{j,i} + r^{j,i}(1-p_d))}. \tag{29}$$

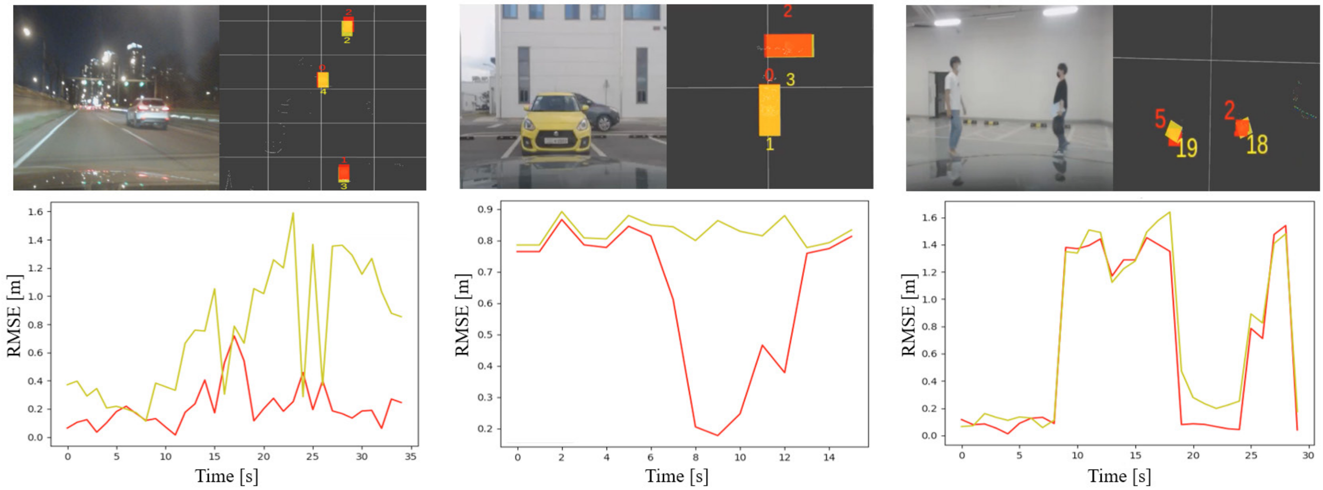

(a) Highway (b) Occluded vehicles (c) Overlapping pedestrians

Fig. 2. The results of three different scenarios. The proposed method and the Kalman filter are indicated in red and yellow, respectively. (a) on the highway at night. (b) vehicles that are occluded in a parking lot. (c) overlapping pedestrians in a parking lot. Each includes a part of the webcam image on the left, a qualitative tracking result on the right, and a calculated RMSE graph with a time axis below.

according to (27). The newly detected targets' cost, c_n is $\rho^u(z)$ calculated by (20). The PMBM discovers the best K hypotheses by employing Murty's algorithm Lu and Rosenbaum (2004) using the created cost matrix.

Estimation Selecting an optimum estimator gives a better estimation output in multi-object tracking. In this paper, we choose a global hypothesis with the highest weight as an estimation output.

$$j^* = \underset{j}{\operatorname{argmax}} \prod_{i=1}^{n} w_{j,i}. \tag{30}$$

Reduction Managing computing complexity and preserving real-time performance necessitates reducing the number of hypotheses. Pruning, capping, gating, recycling, and merging methods are used in the implementation of this paper. Additional details of each method can be found in the García-Fernández et al. (2018).

4. EXPERIMENTS

The proposed method has been evaluated by an actual vehicle with heterogeneous and asynchronous sensors: a camera in the front of the vehicle, scanning LiDAR, and electronically scanning radar in the front and rear. With its specific data frequency, each sensor provides its clustering output. They are synchronized and corrected using short-term prediction to be used in the centralized architecture. Aside from the sensors used in the fusion, there are three high-end 3D scanning LiDARs on the top.

For evaluation, we used the clustering outputs of LiDAR-based verification sensors that were not employed in multi-sensor fusion as ground truth since there was no accurate ground truth in the actual vehicle dataset. The Root Mean Square Error and the number of ID switches are utilized as evaluation metrics, and a Kalman filter tracker (KF) with score-based track management is employed for the comparison.

Although various situations have been verified, Fig. 2 contains three scenarios around 30 seconds long; one common highway situation and two challenging situations for vehicles and pedestrians.

When compared to the verification sensor qualitatively, both trackers show similar performances in (a) of Fig. 2. However, unlike the KF, which uses an empirical track birth and death management, the track birth method of the proposed method based on the Poisson RFS allows faster track generation of the proposed method. The quantitative evaluation shows an unstable shape because of the poor clustering of the verification sensor, but the RMSE of the proposed method is lower than that of the comparative group in most cases, as shown in Fig. 2 and Table 2. In a situation when a car passes behind a car in the parking lot and completely covers it for a while, our method shows significantly less error than the KF.

For urban autonomous driving, not only vehicle tracking but also pedestrian tracking is essential, and a detailed explanation of the challenging urban scenario (c) will be given below. For scenario (c) of Fig. 2, two pedestrians in the parking lot overlap at the view of the automotive vehicle. Their top-view trajectories are illustrated in (c) of Fig. 3. As shown in (d) of Fig. 3, the KF is unable to maintain track continuity after overlapping. In (a) of Fig. 3, the track ID of a pedestrian on the right turns from 18 to 23. However, due to the probabilistic hypotheses of the proposed method against the KF, the proposed method preserves track continuity in challenging scenarios. It can be considered a significant advantage in multi-object tracking.

Table 2. Average RMSE comparison of Fig. 2

Average RMSE	Proposed method	Kalman filter
Scenario (a)	**0.2180**	0.7345
Scenario (b)	**0.5677**	0.8440
Scenario (c)	**0.6592**	0.7617

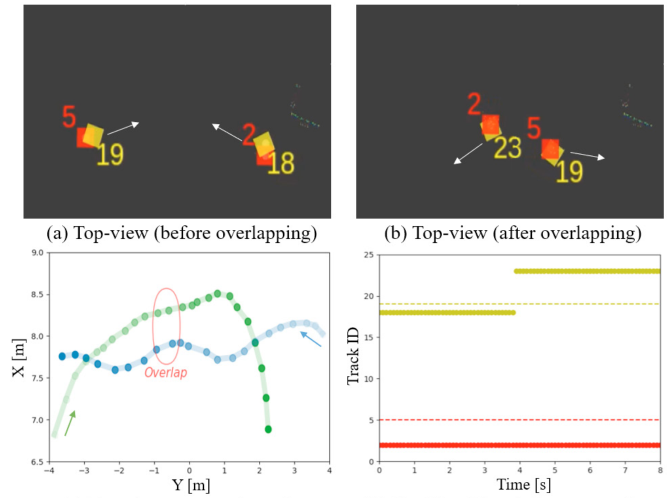

(a) Top-view (before overlapping) (b) Top-view (after overlapping)

(c) Top-view target trajectories (d) Tracking ID switches comparison

Fig. 3. The results of scenarios (c) of Fig. 2. The proposed method and the Kalman filter are indicated in red and yellow, respectively. Tracking results before and after overlapping are shown in (a) and (b). (c) illustrates the whole top-view trajectory of pedestrians throughout the scenario, with arrows indicating their beginning places. The tracking ID switch comparison for both methods is shown in (d).

5. CONCLUSION

The Random Finite Set tracker, unlike the frequently used Kalman filter tracker, can directly model the number of objects. Among the Random Finite Set based approaches, the Poisson Multi-Bernoulli Mixture filter performs well. Based on this, we propose a centralized multi-sensor tracker for autonomous driving applications using the Poisson Multi-Bernoulli Mixture filter. The tracker fuses heterogeneous automotive sensors while accounting for data uncertainties. We present a real-world vehicle evaluation in comparison to a Kalman filter tracker. The proposed method outperforms the Kalman filter tracker in challenging scenarios, according to the experimental results. There are several possible themes to investigate for future work, including the evaluation of publicly available datasets and the development of multiple motion models and a decentralized architecture.

ACKNOWLEDGEMENTS

This work was supported by the Industrial Strategic Technology Development Program (10079730, Development and Evaluation of Automated Driving Systems for Motorway and City Road) funded By the Ministry of Trade, Industry & Energy (MOTIE, Korea).

REFERENCES

Bar-Shalom, Y., Daum, F., and Huang, J. (2009). The probabilistic data association filter. *IEEE Control Systems Magazine*, 29(6), 82–100. doi: 10.1109/MCS.2009.934469.

Fröhle, M., Granström, K., and Wymeersch, H. (2018). Multiple target tracking with uncertain sensor state applied to autonomous vehicle data. In *2018 IEEE Statistical Signal Processing Workshop (SSP)*, 628–632. IEEE.

Frossard, D. and Urtasun, R. (2018). End-to-end learning of multi-sensor 3d tracking by detection. In *2018 IEEE International Conference on Robotics and Automation (ICRA)*, 635–642. doi:10.1109/ICRA.2018.8462884.

García-Fernández, Á.F., Williams, J.L., Granström, K., and Svensson, L. (2018). Poisson multi-bernoulli mixture filter: direct derivation and implementation. *IEEE Transactions on Aerospace and Electronic Systems*, 54(4), 1883–1901.

Hall, D. and Llinas, J. (1997). An introduction to multisensor data fusion. *Proceedings of the IEEE*, 85(1), 6–23. doi:10.1109/5.554205.

Liu, H., Fang, S., and Jianhua, J. (2020). An improved weighted fusion algorithm of multi-sensor. In *Journal of Physics: Conference Series*, volume 1453, 012009. IOP Publishing.

Lu, B. and Rosenbaum, P. (2004). An algorithm for ranking all the assignments in order of increasing cost. *Journal of Computational and Graphical Statistics*, 13(2), 422–434.

Mahler, R.P. (2007). *Statistical multisource-multitarget information fusion*, volume 685. Artech House Norwood, MA, USA.

Pang, S., Morris, D., and Radha, H. (2021). 3d multi-object tracking using random finite set-based multiple measurement models filtering (rfs-m 3) for autonomous vehicles. In *2021 IEEE International Conference on Robotics and Automation (ICRA)*, 13701–13707. IEEE.

Pang, S. and Radha, H. (2021). Multi-object tracking using poisson multi-bernoulli mixture filtering for autonomous vehicles. In *ICASSP 2021-2021 IEEE International Conference on Acoustics, Speech and Signal Processing (ICASSP)*, 7963–7967. IEEE.

Reid, D. (1979). An algorithm for tracking multiple targets. *IEEE transactions on Automatic Control*, 24(6), 843–854.

Scheidegger, S., Benjaminsson, J., Rosenberg, E., Krishnan, A., and Granström, K. (2018). Mono-camera 3d multi-object tracking using deep learning detections and pmbm filtering. In *2018 IEEE Intelligent Vehicles Symposium (IV)*, 433–440. doi:10.1109/IVS.2018.8500454.

Thanh, L.B., Alexandrovich, P.D., and Ruben, P. (2021). Multi-object multi-sensor tracking simulation using poisson multi-bernoulli mixture filter. In *2021 23rd International Conference on Digital Signal Processing and its Applications (DSPA)*, 1–6. IEEE.